ORGANIC CHEMISTRY

The total synthesis of (−)-spiroaspertrione A: A divinylcyclopropane rearrangement approach

Wenbo Huang[1,2]†, Lu Pan[1,2]†, Heng Zhao[3], Fabian Schneider[1]*, Tanja Gaich[2]*

The rise of multidrug-resistant pathogens poses a major threat to global health, with methicillin-resistant *Staphylococcus aureus* (MRSA) among the most challenging. One promising approach to overcoming resistance is using small molecules that resensitize MRSA to existing drugs. Here, we report the enantioselective total synthesis of one such promising candidate, (−)-spiroaspertrione A, a complex meroterpenoid of the andiconin family. This natural product has long eluded synthesis because of its densely functionalized polycyclic backbone. Our route features a stereoselective Diels-Alder cycloaddition, followed by a key divinylcyclopropane rearrangement forming the spirobicyclo[3.2.2]nonane core, which proved to be reversible and was further investigated by density functional theory calculations. Strategic late-stage functionalization of the compact cage architecture enabled access to the natural product and provided evidence for a plausible biosynthetic relationship with (−)-aspermerodione.

The structural diversity and complexity of fungal meroterpenoids arise primarily from the catalytic versatility of various enzymes that orchestrate reactions with distinct patterns and stereospecificity at multiple stages of biosynthesis, leading to pathway divergence. Since the isolation of the first 3,5-dimethylorsellinic acid (DMOA)–derived meroterpenoid, andibenin B (**1**) (*1*), in 1976 from *Aspergillus variecolor*, >200 secondary metabolites have been identified in this category (*2*–*4*). These compounds share a common polyketide origin but diverge considerably through distinct terpene coupling and tailoring reactions. Among them, a defined subgroup features andiconin (**2**) (*5*), which serves as a gateway compound to a series of closely related yet architecturally diverse natural products (Fig. 1A, **1** to **6**). One prominent example is (−)-spiroaspertrione A (**3**) (*6*), first isolated in 2017 from a culture of *Aspergillus* sp. TJ23. Subsequent biological evaluations revealed that (−)-spiroaspertrione A (**3**) exhibits potent activity against methicillin-resistant *Staphylococcus aureus* (MRSA), with a minimum inhibitory concentration (MIC) value of 4 μg/ml. Additionally, (−)-spiroaspertrione A (**3**) resensitizes MRSA to oxacillin, reducing its MIC value against MRSA from 32 to 1 μg/ml (*6*). Despite this marked bioactivity, further in vivo evaluation and mechanistic studies were hindered by the limited amount of material available from the fungus *Aspergillus*. This scarcity (10.5 mg of **3** isolated from 25 liters of culture), combined with the lack of synthetic access to the andiconin-derived meroterpenoids, underscores the value of (−)-spiroaspertrione A (**3**) as a synthetic target.

[1]Shanghai Research Center for Bioactive Molecule Synthesis (BiMoS), Shanghai University of Traditional Chinese Medicine, Shanghai, China. [2] Department of Chemistry, University of Konstanz, Konstanz, Germany. [3] Department of Chemistry, University of Fribourg, Fribourg, Switzerland. ***Corresponding author. Email: fschneider@shutcm.edu.cn (F.S.); tanja.gaich@uni-konstanz.de (T.G.)** †These authors contributed equally to this work.

In contrast to the more common tricyclo[4.3.1.0^{3,7}]decane and tricyclo[4.3.1.0^{3,8}]decane frameworks typically found in andiconin-derived meroterpenoids (Fig. 1A, green and blue, respectively), (−)-spiroaspertrione A (**3**) features a spirobicyclo[3.2.2]nonane core (red), which presents several synthetic challenges. Foremost among these is the construction of the spirobicyclic scaffold bearing adjacent quaternary centers at C8 and C2′, which requires overcoming substantial steric hindrance. Furthermore, functionalization of the core is impeded by stereoelectronic interactions along the cage periphery and by the presence of the vicinal C9 ketone moiety. Another congener, (−)-aspermerodione (**4**) (*7*), which shares the same carbon skeleton as (−)-spiroaspertrione A (**3**), also captured our attention. Despite its distinct molecular geometry, (−)-aspermerodione (**4**) exhibits comparable biological activity to (−)-spiroaspertrione A (**3**) (*7*), albeit with slightly reduced potency, suggesting the involvement of a common bioactive intermediate and a shared mode of action, as well as the possibility of interconversion. This hypothesis is supported by Matsuda and Abe's proposal (*8*), that (−)-aspermerodione (**4**) is a downstream biosynthetic intermediate of (−)-spiroaspertrione A (**3**) (Fig. 1B) that is formed through hydrolysis and methylation. Inspired by this insight, our retrosynthetic analysis envisioned accessing (−)-spiroaspertrione A (**3**) through a transannular elimination of methanol from (−)-aspermerodione (**4**) (blue arrows). Our synthetic route to (−)-aspermerodione (**4**) used a divinylcyclopropane rearrangement (DVCPR) (*9*, *10*) of (***E***)-**8** to assemble the spirobicyclo[3.2.2]nonane core in **7**. The precursor (***E***)-**8** was delineated from diene **9**, wherein the C8 spiro center was constructed stereoselectively through an intermolecular Diels-Alder cycloaddition between diene **10** and enone **11**.

Route to the divinylcyclopropane intermediate

Our synthesis commenced with (+)-enoxolone (**12**), an inexpensive (0.90 euros/g) chiral pool building block. After Jones oxidation of **12** to ketone **13**, flash vacuum pyrolysis triggered a *retro*-Diels-Alder reaction that directly afforded bicyclic building block **14** (*11*), which was converted to the literature-known enone **11** through four functional group interconversions. A Diels-Alder cycloaddition between enone **11** and diene **10** established the C8 spiro center. The best results were obtained using Jung's mixed Lewis acid catalysis [Al(CH$_3$)$_3$–AlBr$_3$] (*12*), followed by oxidation with 2,3-dichloro-5,6-dicyano-1,4-benzoquinone (DDQ) (*13*), yielding spiroenone **15** with excellent diastereomeric

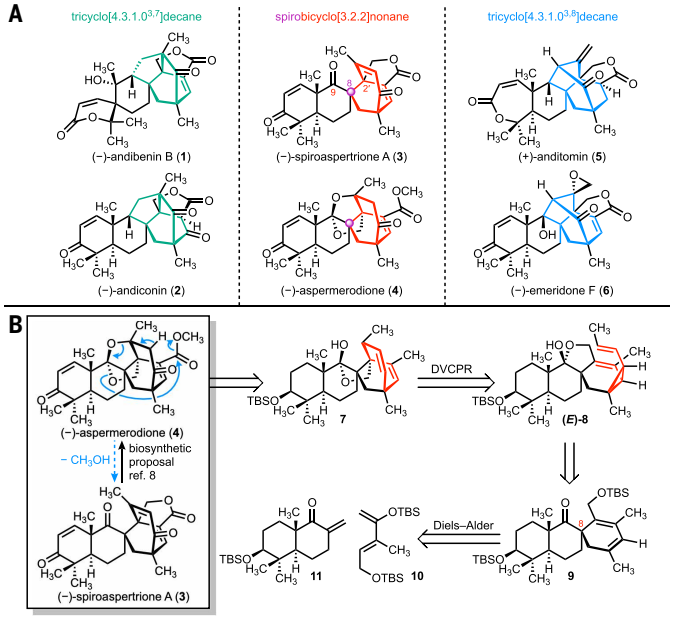

Fig. 1. Andiconin-derived meroterpenoids. (**A**) Representative natural products. (**B**) Retrosynthetic analysis of (−)-spiroaspertrione A (**3**). TBS, *tert*-butyldimethylsilyl.

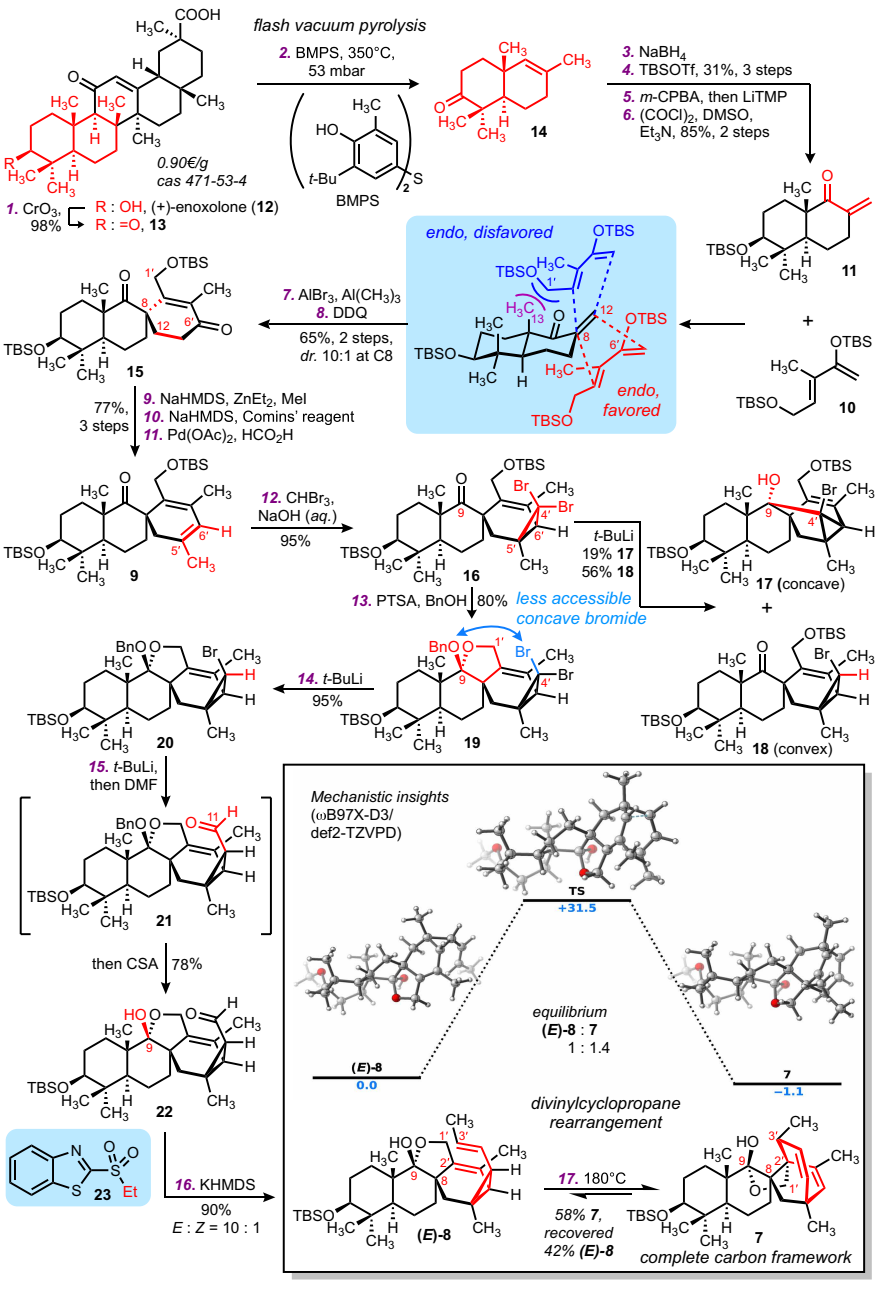

Fig. 2. Construction of the carbon framework through DVCPR. Reagents and conditions: (1) CrO_3, acetone, 0°C; (2) 4,4′-thiobis(2-methyl-6-*tert*-butylphenol) (BMPS), 350°C, 53 mbar; (3) $NaBH_4$, tetrahydrofuran (THF)–CH_3OH (3:1), 0°C; (4) *tert*-butyldimethylsilyl triflate (TBSOTf), triethylamine (Et_3N), CH_2Cl_2, 0°C; (5) *meta*-chloroperoxybenzoic acid (*m*-CPBA), $NaHCO_3$, 0°C, then lithium tetramethylpiperidide (LiTMP), THF, 0°C; (6) $(COCl)_2$, DMSO, Et_3N, −78°C to room temperature (RT); (7) $Al(CH_3)_3$, $AlBr_3$, CH_2Cl_2, −15°C, diastereomeric ratio 10:1 at C8); (8) DDQ, lutidine, toluene, RT; (9) sodium bis(trimethylsilyl)amide (NaHMDS), THF, 0°C, then diethylzinc ($ZnEt_2$), 1,3-dimethyl-3,4,5,6-tetrahydro-2(1*H*)-pyrimidinone (DMPU), CH_3I; (10) NaHMDS, THF, 0°C, then *N*-(5-chloropyridin-2-yl)-1,1,1-trifluoro-*N*-((trifluoromethyl)sulfonyl)methanesulfonamide (Comins' reagent); (11) palladium(II) acetate $Pd(OAc)_2$, triphenylphosphine (PPh_3), Et_3N, HCO_2H, THF, 70°C; (12) $CHBr_3$, benzyltriethylammonium chloride (TEBAC), NaOH (50 wt% aq.), RT; (13) PTSA, benzyl alcohol (BnOH), 4Å molecular sieves, toluene, RT; (14) *tert*-butyllithium (*t*-BuLi), THF, −78°C; (15) *t*-BuLi, −78 to 0°C, then −78°C, DMF, then CSA, RT; (16) 2-ethylsulfonyl-1,3-benzothiazole (**23**), potassium bis(trimethylsilyl)amide (KHMDS), THF, −78°C; and (17) toluene, 180°C. Mechanistic insights into the DVCPR are from DFT calculations. Energies (in kcal/mol) are relative to that of **(*E*)-8**, and all structures were calculated at the (ωB97X-D3/def2-TZVPD||BP86-D3BJ/def2-SVP) level of DFT.

control at the C8 spiro center (diastereomeric ratio, 10:1). This stereoselectivity was attributed to steric interactions between the C13 angular methyl group (Fig. 2, first blue box, highlighted in purple) and diene **10** in the transition state, as illustrated by two distinct orientations (highlighted in blue and red). Proceeding from enone **15**, α-methylation of the C6′ ketone was facilitated by $ZnEt_2$ (*14*, *15*), which minimized the basicity of the enolate and thus suppressed undesired α-dimethylation. Subsequent vinyl triflate formation using Comins' reagent followed by reductive detriflation yielded diene **9**. Next, various approaches were explored to construct divinylcyclopropane, including the classic combination of diazo compounds with transition metal catalysis (e.g., rhodium or copper) (*16*). However, the low reactivity of the C5′–C6′ trisubstituted olefin in **9** thwarted these attempts, resulting in recovery of the starting material. Nevertheless, cyclopropanation of **9** using dibromocarbene (*17*, *18*) provided dibromocyclopropane **16** in 95% yield as a single diastereomer.

Stereoselective lithium-bromine exchange on the gem-dibromocyclopropane **16** afforded the desired monobromide **18** in a 3:1 ratio, with tertiary alcohol **17** resulting from intramolecular addition of the C4′ concave carbanion to the C9 ketone. Extensive studies of this lithium-bromine exchange revealed that the C4′ cyclopropyl carbanion was configurationally stable, thus suggesting that the 3:1 ratio of bromide **18** and alcohol **17** reflects the kinetic rates of the lithium-bromide exchange between the convex and concave bromide substituents. To suppress the unwanted aldol addition, the C9 carbonyl in **16** was protected as acetal **19**, which also exerted concave or convex kinetic differentiation through steric interactions. Indeed, treatment of **19** with *tert*-butyllithium furnished the convex debromination product **20** as a single diastereomer. Further treatment of **20** with *tert*-butyllithium, followed by dimethylformamide (DMF) and camphorsulfonic acid (CSA), sequentially generated aldehyde **21** and hydrolyzed the C9 ketal in situ to afford hemiketal **22**. A modified Julia olefination (*19*) between aldehyde **22** and benzothiazole sulfone **23** provided **(*E*)-8** in 90% yield as a 10:1 mixture of (*E*) and (*Z*) isomers. Hydrolysis of the C9 benzyl ketal before the olefination was crucial for achieving high *E*/*Z* selectivity, because direct olefination of **21** under identical conditions gave poor stereoselectivity (*E*:*Z* = 1.4:1).

DVCPR and density functional theory calculations

Heating of **(*E*)-8** at 180°C established an equilibrium between it and the desired DVCPR product, **7** (1:1.4). This intermediate contains the complete carbon framework of (−)-spiroaspertrione A (**3**), comprising six contiguous stereogenic centers including three quaternary centers. Typically, DVCPR is an irreversible process because of the significant energy difference between the starting material and the product. However, in the

case of (***E***)-**8**, the energy released upon cyclopropane ring opening (~27 kcal/mol) is mitigated by the formation of the two adjacent quaternary centers C8 and C2′ in **7**, resulting in a marginal energy difference between (***E***)-**8** and **7**. Density functional theory (DFT) calculations (wB97X-D3/def2-TZVPD||BP86-D3BJ/def-SVP; see the supplementary materials) were used to study this equilibrium. The activation energy required for this transformation was determined to be 31.5 kcal/mol, consistent with the high experimental temperature (180°C), whereas the energy difference between **7** and (***E***)-**8** was only −1.1 kcal/mol, leading to the observed equilibrium.

Late-stage functionalization: Completion of the synthesis

Upon obtaining the DVCPR product **7**, our final objective was to establish the oxidation patterns at C3′, C4′, and C8′ of the bicyclic core and C1, C2, and C3 at the decalin moiety (Fig. 3A). However, attempts to introduce oxidation or desaturation at the C3′ position of **7** proved to be challenging. Several strategies were explored to address this hurdle. One approach leveraged the spatial proximity of the C9 hemiketal and C3′–H, as evidenced by nuclear Overhauser effect (NOE) studies and the formation of the bicyclic ketal in (−)-aspermerodione (**4**). Heating hemiketal **7** with lead tetraacetate in benzene at reflux temperature (*20*, *21*) achieved the desired intramolecular hydrogen abstraction, yielding bicyclic ketal **24**. However, the formation of the C3′ oxygen bridge deactivated the C11–C4′ double bond, impeding further progress. Treatment of ketal **24** with Schlosser's base (*n*-BuLi–KO*t*-Bu) (*22*–*24*) induced deprotonation at the C8′ allylic position, triggering a substantial skeletal rearrangement (Fig. 3A, blue arrows) that afforded barbaralane **25** quantitatively. However, attempts to convert alkene **25** into allylic alcohol **26** through Mukaiyama hydration (*25*) led to decomposition of the material.

In light of this observation, we prioritized the oxidation of the C11–C4′ double bond and aimed to desaturate the C3′ position using a Saegusa-Ito oxidation (*26*) of the C4′ ketone (Fig. 3B). Alkene **7** underwent allylic oxidation with selenium dioxide to the allylic alcohol **27**, which could then be further oxidized to lactone **28** quantitatively with manganese dioxide. The introduction of the C4′ ketone was achieved by a sequence comprising epoxidation of the C11–C4′ double bond of **28** with dimethyldioxirane (DMDO), titanium(III)–mediated reductive epoxide opening, and oxidation of the C4′ alcohol under Ley's conditions (*27*). Unfortunately, attempts to desaturate C3′–C11 within **31** using 2-iodoxybenzoic acid (IBX) or DDQ were unsuccessful. The C4′ ketone could be transformed into the corresponding silyl enol ether but failed to undergo further oxidation (Fig. 3B). In addition to the expected alcohol **30**, an unorthodox by-product, cyclobutanol **29**, bearing a new tricyclo[4.2.1.$0^{3,8}$]nonane core, was formed from the reductive epoxide opening by an intramolecular radical Michael addition (from C11 to C6′). This observation illustrates the close proximity of the cage periphery, which repeatedly led to unexpected chemical behavior of the cage system.

To circumvent these issues, we focused on generating the C11–C4′ epoxide with the intent to convert it into an allylic alcohol through the intermediacy of a selenohydrin (Fig. 4A). Treatment of alkene **7** with DMDO provided a diastereomeric mixture of epoxides ***32*** and ***33***. The subsequent reaction with lithium phenylselenide (PhSeLi) not only produced the expected selenohydrins ***34*-Se** and ***35*-Se**, but also directly yielded allylic alcohol **26** in moderate yield. Analyzing the results and conditions led to the conclusion that the desired allylic alcohol **26** was generated from epoxide ***33***, with PhSeLi acting primarily as a bulky base in this transformation.

The reaction was subsequently optimized to increase the selectivity for the formation of ***33***. After extensive screening (seen in Fig. 4, table 1), we determined that protic solvents capable of hydrogen bonding, such as methanol, increased the amount of ***33***. The origin of this diastereoselectivity was rationalized as arising from hydrogen bonding

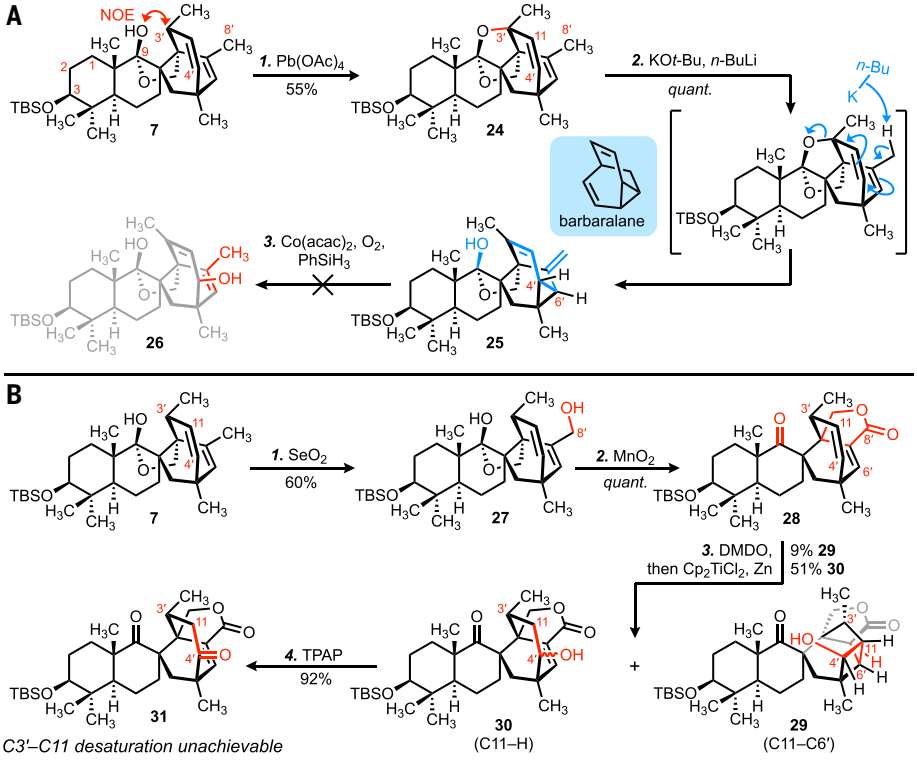

Fig. 3. Attempts to oxidize or desaturate the C3′ position. (**A**) Intramolecular hydrogen abstraction. Reagents and conditions: (1) lead tetraacetate [$Pb(OAc)_4$], benzene, 90°C; (2) potassium *tert*-butoxide (KO*t*-Bu), *n*-butyllithium (*n*-BuLi), THF, −78°C; (3) cobalt(II) acetylacetonate [$Co(acac)_2$], phenylsilane ($PhSiH_3$), O_2 (balloon), RT. (**B**) Saegusa-Ito oxidation. Reagents and conditions: (1) selenium dioxide (SeO_2), 1,4-dioxane–pyridine (2:1), 80°C; (2) manganese dioxide (MnO_2), CH_2Cl_2, RT; (3) DMDO, CH_2Cl_2, 0°C, then titanocene dichloride (Cp_2TiCl_2), Zn^0, triethylsilane (Et_3SiH), THF, −78°C to RT; and (4) tetrapropylammonium perruthenate (TPAP), CH_2Cl_2, 0°C.

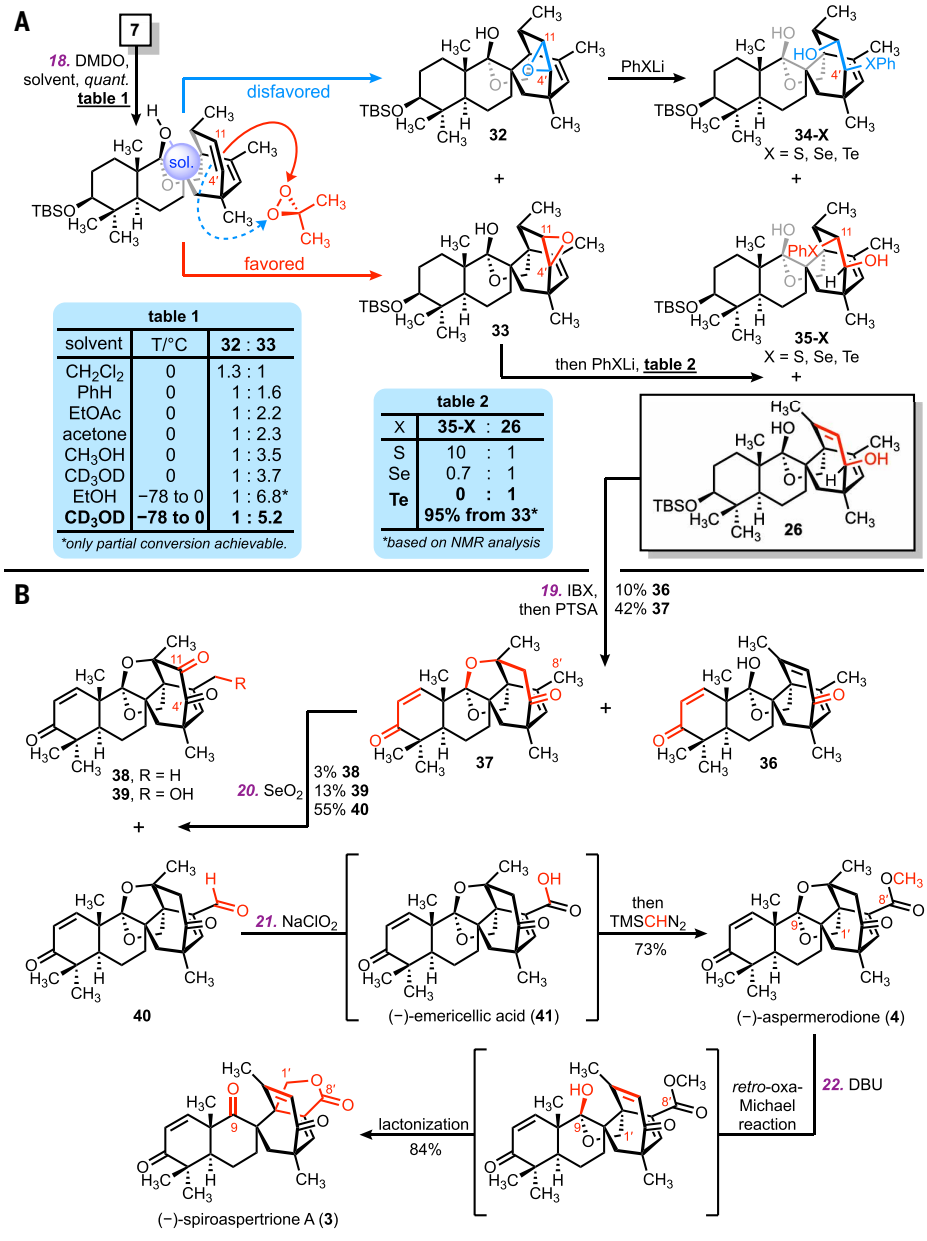

Fig. 4. Late-stage functionalizations. (**A**) Preparation of allylic alcohol **26** through epoxide **30**. Reagents and conditions (step count continued from Fig. 2): (18) DMDO, then lithium phenyltelluride (PhTeLi), 90°C. (**B**) Synthesis of (−)-spiroaspertrione A (**3**). Reagents and conditions: (19) 2-IBX, DMSO, RT, then PTSA, 70°C; (20) SeO_2, 1,4-dioxane, 120°C; (21) sodium chlorite ($NaClO_2$), monosodium phosphate (NaH_2PO_4), 2-methyl-2-butene, *t*-BuOH–THF–H_2O (1:2:1), 0°C, then trimethylsilyldiazomethane ($TMSCHN_2$); and (22) DBU, benzene, 100°C.

between the C9 hemiketal and the protic solvent, which serves to occlude the approach of DMDO to the undesired face of the C11–C4′ alkene. Therefore, using appropriately sized alcohols and lower temperatures should in principle favor the formation of epoxide ***33***. Indeed, deuterated methanol slightly improved the results, whereas lowering the temperature significantly boosted the ratio of ***33*** to ***32***. Even better diastereoselectivity was observed in ethanol, but its vulnerability to DMDO oxidation made full conversion challenging to achieve. To increase the amount of **26**, we varied the base (Fig. 4A and table S2). Heating ***33*** with lithium phenyltelluride (PhTeLi) at 90°C generated **26** as the sole product in almost quantitative yield, whereas lithium phenylthiolate (PhSLi) predominantly produced **35-S**.

The allylic alcohol **26** was oxidized with IBX in dimethyl sulfoxide (DMSO) in the presence of para-toluenesulfonic acid (PTSA) (*28*) to provide enone **36** and the bicyclic ketal **37**. Allylic oxidation of the C8′ methyl group of **37** was performed with selenium dioxide, yielding aldehyde **40**, along with **38** and **39**, arising from Riley oxidation (*29*) of the ketone C4′. The pronounced tendency for enolization at the C11 position, however, supported our earlier hypothesis regarding the cascade transformation from (−)-aspermerodione (**4**) to (−)-spiroaspertrione A (**3**). The preparation of **4** was achieved from aldehyde **40** through Pinnick oxidation (*30*) and trapping of the in situ generated (−)-emericellic acid (**41**) using $TMSCHN_2$. As hypothesized, heating with 1,8-diazabicyclo[5.4.0]undec-7-ene (DBU) at 100°C triggered a *retro*-oxa-Michael reaction, leading to the collapse of the C9 hemiketal and liberating the C1′ primary alcohol, which subsequently attacked the C8′ methyl ester, thus forming the lactone moiety of (−)-spiroaspertrione A (**3**). The optical rotations of both synthetic

natural products **3** and **4** matched the values reported in the literature (*6*, *7*).

Conclusions

We accomplished the enantioselective total synthesis of an andiconin-derived meroterpenoid, (−)-spiroaspertrione A (**3**), in 16 steps from the literature-reported compound **11** with an overall yield of 2.3%. This achievement allowed us to study the previously hypothesized interconversion between (−)-spiroaspertrione A (**3**) and (−)-aspermerodione (**4**). The synthesis also granted us broader insight into the relationship between the more common frameworks of the andiconin family.

REFERENCES AND NOTES

1. A. W. Dunn, R. A. W. Johnstone, B. Sklarz, T. J. King, *J. Chem. Soc. Chem. Commun.* **270**, 270a (1976).
2. R. Geris, T. J. Simpson, *Nat. Prod. Rep.* **26**, 1063–1094 (2009).
3. Y. Matsuda, I. Abe, *Nat. Prod. Rep.* **33**, 26–53 (2016).
4. M. Jiang, Z. Wu, L. Liu, S. Chen, *Org. Biomol. Chem.* **19**, 1644–1704 (2021).
5. Y. Matsuda, T. Wakimoto, T. Mori, T. Awakawa, I. Abe, *J. Am. Chem. Soc.* **136**, 15326–15336 (2014).
6. Y. He *et al.*, *J. Org. Chem.* **82**, 3125–3131 (2017).
7. Y. Qiao *et al.*, *Sci. Rep.* **8**, 5454 (2018).
8. T. Bai *et al.*, *Org. Lett.* **22**, 4311–4315 (2020).
9. E. Vogel, *Angew. Chem.* **72**, 4–26 (1960).
10. E. Vogel, K. H. Ott, K. Gajek, *Justus Liebigs Ann. Chem.* **644**, 172–188 (1961).
11. J. R. Falck, S. Manna, S. Chandrasekhar, L. Alcaraz, C. Mioskowski, *Tetrahedron Lett.* **35**, 2013–2016 (1994).
12. M. E. Jung, D. Ho, H. V. Chu, *Org. Lett.* **7**, 1649–1651 (2005).
13. I. Ryu, S. Murai, Y. Hatayama, N. Sonoda, *Tetrahedron Lett.* **19**, 3455–3458 (1978).
14. Y. Morita, M. Suzuki, R. Noyori, *J. Org. Chem.* **54**, 1785–1787 (1989).
15. E. L. Fisher, S. M. Wilkerson-Hill, R. Sarpong, *J. Am. Chem. Soc.* **134**, 9946–9949 (2012).
16. H. M. Davies, E. Saikali, W. B. Young, *J. Org. Chem.* **56**, 5696–5700 (1991).
17. W. von E. Doering, A. K. Hoffmann, *J. Am. Chem. Soc.* **76**, 6162–6165 (1954).
18. M. Mąkosza, M. Wawrzyniewicz, *Tetrahedron Lett.* **10**, 4659–4662 (1969).
19. J. B. Baudin, G. Hareau, S. A. Julia, O. Ruel, *Tetrahedron Lett.* **32**, 1175–1178 (1991).
20. K. Heusler, J. Kalvoda, *Angew. Chem. Int. Ed.* **3**, 525–538 (1964).
21. M. L. Mihailović, Ž. Čeković, *Synthesis (Stuttg.)* **1970**, 209–224 (1970).
22. K. Fujita, M. Schlosser, *Helv. Chim. Acta* **65**, 1258–1263 (1982).
23. M. Schlosser, *Pure Appl. Chem.* **60**, 1627–1634 (1988).
24. A. Zech, C. Jandl, T. Bach, *Angew. Chem. Int. Ed.* **58**, 14629–14632 (2019).
25. S. Isayama, T. Mukaiyama, *Chem. Lett.* **18**, 1071–1074 (1989).
26. Y. Ito, T. Hirao, T. Saegusa, *J. Org. Chem.* **43**, 1011–1013 (1978).
27. S. V. Ley, J. Norman, W. P. Griffith, S. P. Marsden, *Synthesis (Stuttg.)* **1994**, 639–666 (1994).
28. K. C. Nicolaou, T. Montagnon, P. S. Baran, *Angew. Chem. Int. Ed.* **41**, 993–996 (2002).
29. H. L. Riley, J. F. Morley, N. A. C. Friend, *J. Chem. Soc.* 1875–1883 (1932).
30. B. S. Bal, W. E. Childers Jr., H. W. Pinnick, *Tetrahedron* **37**, 2091–2096 (1981).
31. W. Huang, L. Pan, H. Zhao, F. Schneider, T. Gaich, Data for: The total synthesis of (−)-spiroaspertrione A: A divinylcyclopropane rearrangement approach, Zenodo (2025); https://doi.org/10.5281/zenodo.16889403.

ACKNOWLEDGMENTS

We thank J. R. Falck (UT Southwestern, Dallas), S. Chandrasekhar (GITAM, Hyderabad), and S. Kallepu (Moffitt Cancer Center) for granting us their original experimental procedure for the flash vacuum pyrolysis; S. B. Herzon (Yale University) and D. Sarlah (Rice University) and H. Zhao and S. Ma (University of Konstanz) for helpful discussions during the project; M. Kovermann, A. Friemel, and U. Haunz (NMR department of the University of Konstanz) for assistance with NMR spectroscopy; M. Bein (University of Konstanz) for assistance with high-resolution mass spectroscopy; and the staff of the SCCKN (Scientific Computer Cluster in Konstanz) at the University of Konstanz for HPC resources. **Funding:** This work was supported by the European Research Council (ERC-consolidator grant ERC-COG-CoSyMoDe, "Cooperative Synthesis by Molecular Deconvolution," grant no. 101003072 to T.G.) and Shanghai University of Traditional Chinese Medicine (Shanghai Bay talent program and research start-up fund for introduced talents to F.S.). **Author contributions:** Conceptualization: T.G., F.S.; Data collection: W.H.; DFT calculations: H.Z.; Funding acquisition: T.G.; Investigation: W.H., F.S.; Writing – original draft: F.S.; Writing – review & editing: F.S., T.G., W.H., L.P.; Writing – supporting information: W.H. **Competing interests:** The authors declare no competing interests. **Data and materials availability:** All data are available in the main text or the supplementary materials. Free induction decay values of NMR spectra of compounds **3**, **4**, **7**, **(*E*)-8**, **17**, **22**, **24**, **25**, **26**, **28**, **37**, and **40** are accessible at Zenodo (*31*).

SUPPLEMENTARY MATERIALS

science.org/doi/10.1126/science.adz7593
Materials and Methods; Spectral Data; References (*32*–*42*)

Submitted 13 June 2025; accepted 21 August 2025

10.1126/science.adz7593